International Journal of Innovative Computing, Information and Control
Volume **8**, Number **11**, November **2012**

ICIC International ©2012 ISSN 1349-4198
pp. 7603–7625

A CROSS-LAYER CONTROL METHOD FOR NETWORK LIFETIME MAXIMIZATION IN WIRELESS SENSOR NETWORKS

Jain-Shing Liu

Department of Computer Science and Information Engineering
Providence University
No. 200, Chung-Chi Rd., Shalu, Taichung 43301, Taiwan
chhliu@pu.edu.tw

Received August 2011; revised February 2012

Abstract. *In this paper, we study the problem of joint routing, scheduling and stream control to maximize the network life, and at the same time, to satisfy end-to-end (ETE) traffic demands in wireless sensor networks (WSNs) with virtual multiple input multiple output (VMIMO) transmission. For this problem, we introduce a cross-layer formulation that can incorporate power and rate adaptation, and seamlessly integrate a SINR constraint at the physical layer to generate feasible sets of links for scheduling at the MAC layer and routing at the network layer. Specifically, we propose a column generation (CG) approach to exactly accommodate the most realistic scenario where power and rate are both discrete. In addition, we develop a fully distributed algorithm using the Lagrangian duality and a subgradient method to allow each node to independently obtain its own lifetime and scheduling parameters for the cross-layer optimization. Finally, we present computational results on different network topologies and discuss the insight to be gained when adopting different parameters on the control method.*
Keywords: Cross-layer design, Lifetime maximization, Wireless sensor networks

1. **Introduction.** A wireless sensor network (WSN) is usually composed of a large number of energy-constraint stations equipped with the capability of sensing, computing and wireless communication, and deployed to detect events of interests and to send data to sink stations. In such a network, sensor stations operate with small batteries that are difficult to replace in typical applications, and thus minimizing its energy consumption poses a considerable challenge to the developers. For this problem, wireless communication has been identified as the dominant power-consumption operation, which continuously intensifies the interest of researchers in the development of energy-efficient wireless transmission schemes. However, the energy issue is mainly devoted to conventional WSNs. In fact, there are different WSNs designed for varied applications requiring our attentions. In this work, we consider the potential that if equipped with the capability of virtual multiple-input multiple-output (VMIMO) realized by, for example, collaborative beamforming (CB) [1], a WSN can have the promise of greatly improving network performance by remarkably increasing transmit power gain and by providing security and interference reduction due to less transmit power being scattered in unintended directions. It had been indicated in [2] that by fixing the power radiated by a given antenna element, ideal transmit beamforming with N antennas can result in a N-fold increased range, an N^2-fold increased rate or an N-fold decrement in the net transmitted power, when compared with single-antenna transmission. An attractive example given there shows that with distributed beamforming, an infeasible signal to noise ratio (SNR) from a single sensor transmission to an overflying aircraft can be increased to provide an upload of image/video data or summarizes of sensor data gathered over days or even months. This

reveals a practical technique for long-haul transmission with power-limited sensors and an adequate solution for building wireless visual sensor networks.

However, the related works for distributed beamforming mainly focus on the characteristics of beampatterns. For example, the work in [1] uses the random array theory along with the assumption of uniformly distributed sensor stations to analyze the CB beampattern. Similarly, the work in [3] uses Gaussian probability density function to model the spatial sensor station distribution in a cluster of WSN, and then uses this model to derive the average beampattern of CB and analyze its characteristics. Despite the beampattern analysis, the cross-layer optimizations proposed so far seldom, if ever, consider the direct impacts of these beampatterns, and further, the corresponding energy consumptions due to the cooperation of sensor stations on the VMIMO-based WSNs. Taking these into account, we pay our attention here to developing a scheme that can cross the layers of physical, MAC, and network, and seamlessly integrate the SINR constraint for generating active sets of VMIMO links. To this end, we formulate the minimum energy cross-layer scheduling as a linear programming (LP) problem with a column generation approach to efficiently select its transmission modes toward an optimal solution.

Apart from the above, we consider also that a distributed algorithm is usually preferred because its centralized counterpart may not work well in a WSN that is a distributed environment by default. Therefore, we next develop a distributed algorithm with a powerful formulation for solving convex optimization problems, namely subgradient method, to get rid of communication overheads and other drawbacks resulting from a centralized approach. Specifically, with this method, the message to be exchanged can be limited within one-hop neighbors of a node, resulting in low communication overheads.

The rest of this paper is organized as follows. In Section 2, we briefly introduce the related works on energy efficiency and network lifetime. Next, in Section 3, we summarize the system model on collaborative beamforming, network communication, and energy consumption. Following that, we present our cross-layer optimization scheme with linear programming in Section 4, and a subgadient-based distributed algorithm in Section 5. Based on the above, a column generation approach for incrementally improving the network lifetime is introduced in Section 6. Finally, the optimization scheme is examined with experiments in Section 7, and our conclusions are drawn in Section 8.

2. **Related Works.**

In the literature, certain research efforts have been done with their aims on reducing energy consumption or maximizing network lifetime. Among these, the approaches with regard to the physical layer could be considered first. For example, the work in [4] summarizes some power control schemes that can reduce the transmission power under a given data rate or error probability. Furthermore, the work in [5] indicates that cooperations among all stations may be required for power control to prevent the situation wherein each station tries to optimize its own SINR value in spite of the network congestion.

The approaches with regard to the MAC layer also receive many attentions. For example, an energy-efficient transmission scheduling problem with constraints on packet deadline and finite buffer is considered in [6], which is then reduced by the authors to a convex optimization problem and solved by an iterative algorithm. In addition, some scheduling algorithms in [7] are proposed to minimize the energy consumption by means of efficient spatial reuse. However, either the power control methods (in the physical layer) or the scheduling algorithms (in the MAC layer) are only energy-efficient approaches specific to their own layers. Consequently, there are research works introduced to seek the cross-layer designs that can concurrently take into account these two layers (PHY and

MAC). For example, a framework for cross-layer design has been proposed in [8] that considers a power control method under the multiple access algorithm used to minimize the transmission power. As another example, a research work in [9] adopts un-coded MQAM as the underlying modulation scheme and a variable-length TDMA scheme as its MAC to minimize the total energy consumption.

Apart from the above, there are other research efforts aiming at cross-layer designs on different layers. For example, the authors in [10] assume that the transmitter power level can be adjusted to use the minimum energy required to reach the intended next hop receiver, and then the energy consumption problem can be reduced to that only depending on the routing decision. Hence, they are able to solve the routing problem with a linear programming approach, and also propose a heuristic, for the network lifetime maximization. Similarly, by considering that the minimum receiver power can be used to determine the required transmission power, the authors in [11] formulate the network lifetime maximization problem as a linear programming problem and propose their distributed iterative algorithms to address the routing problem. Lately, in [12] the authors show that ignoring a bandwidth constraint can lead to infeasible routing, and hence provide optimization models to tackle both energy and bandwidth constraints for a joint design of routing and link rate allocation in WSNs.

More recently, the researchers on this topic intensify their interests in cross-layer designs involving more and more layers. For example, in [13], the authors study the problem of joint routing, link scheduling and power control to support high data rates on WSNs. To this end, they propose an algorithm for link scheduling and power control to minimize the total average energy consumption in such networks. In [14], the authors consider a joint optimal design of physical, MAC, and routing layers to maximize the lifetime of WSNs. Specifically, they use TDMA as their MAC to formulate the optimization problem as a mixed integer convex problem, which can be solved with standard techniques such as interior point methods. Recently, by adopting a pure TDMA as the MAC while using Karush-Kuhn-Tucker (KKT) condition as the model tool, the authors in [15] derive analytical expressions for the network lifetime maximization problem in a small scale planar network, and also suggest an iterative algorithm to obtain suboptimal solutions for a larger such network. In addition, the authors in [16] address the joint design of end-to-end communication rate, power allocation and transmission scheduling for WSNs and develop a column generation approach to yield a sequence of feasible resource allocations.

When compared with the relevant researches, our work to be introduced has its unique characteristics different from the others, as summarized as follows.

- Unlike the previous works [13-16], which usually consider wireless links without cooperative relays, in this work we adopt the distributed beamforming as its transmission scheme to develop a cross-layer formulation that can jointly solve routing, scheduling and stream control problems with the aim of network lifetime maximization while satisfying a given end-to-end (ETE) traffic demand.
- By using the column generation approach designed for this problem, we exactly accommodate the most realistic scenario wherein power and rate are both discrete in contrast with the related works given in [13, 16, 17, 18] that formulate their own problems with only fixed, variable, or partially discrete power and/or rate adaptation.
- Different from the works on wireless multi-hop networks in [8, 10, 18] that focus on centralized approaches, our work also develops a distributed algorithm with a subgradient method that allows each node to independently obtain its own lifetime and scheduling parameters for the optimization.

- Different from our previous work in [19] that aims at the minimum energy scheduling problem (MESP), here we deal with the network lifetime maximization problem as mentioned. To reveal their performance differences on the lifetime, in the experiment, we also compare the two optimizations and show that our objective in this work actually leads to a higher network lifetime in the end, rather than just a low energy consumption as the previous that may not prolong the lifetime after all.

3. System Model.

3.1. Overview of collaborative beamforming.

At the beginning, we concisely introduce the collaborative beamforming (CB) to be adopted, which has been widely considered in, e.g., [1, 3, 20, 21]. To this end, we show in Figure 1 a WSN composed of N randomly located stations in (x, y) plane and organized into k_c clusters or virtual nodes (vnodes). In the WSN, each station has a single antenna operated in a half duplex mode, and its rectangular coordinates, (x_k, y_k), $k \in \{1, \ldots, N\}$, are conveniently represented by its polar counterparts of $\left(r_k = \sqrt{x_k^2 + y_k^2},\ \psi_k = \tan^{-1}\left(\frac{y_k}{x_k}\right)\right)$. Let M_i, $i \in \{1, 2, \ldots, k_c\}$, be a cluster of stations located within the coverage range of its centre and $C_i \subset M_i$ be a set of collaborative stations selected from M_i. To transmit, the source cluster head (CH) that starts transmissions for a user session initialized within its cluster, say CH_i, first broadcasts its data to the cluster members M_i. Then, the $n_i = |C_i|$ cooperative stations (CN) will listen and transmit the data to the next cluster head, say CH_j, $j \in \{1, 2, \ldots, k_c\} \backslash i$ if it is scheduled. In order to construct a main lobe towards CH_j, the carrier of each should be synchronized with initial phase $\Psi_k = -\frac{2\pi}{\lambda} d_k(\varphi_j)$, where λ denotes the wavelength and $d_k(\phi) \approx A - r_k \cos(\phi - \psi_k)$ is the Euclidean distance between the k^{th} station and a point (A, ϕ) at the reference sphere $r = A$. With that, the array factor corresponding to the stations in C_i can be given by [20]

$$F(\phi/C_i) = \frac{1}{n_i} \sum_{k \in C_i} e^{\Psi_k} e^{j \frac{2\pi}{\lambda} d_k(\phi)} \tag{1}$$

where $1/n_i$ is the normalization factor used to distinguish between gains coming from increased overall transmit power and gains from cooperation. Then, with the array factor, the far-field beampattern would be defined as [1]

$$P(\phi/C_i) \stackrel{\triangle}{=} |F(\phi/C_i)|^2 \tag{2}$$

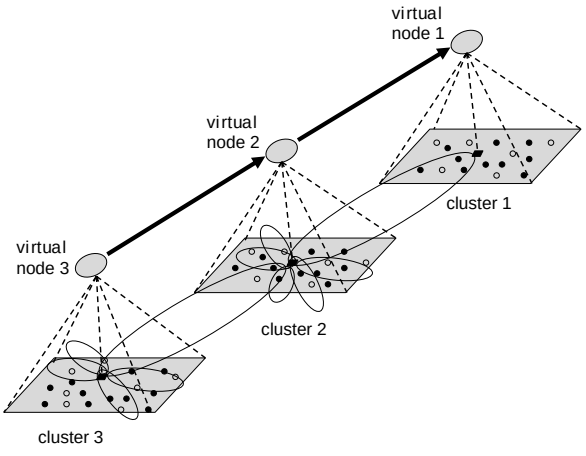

FIGURE 1. Multi-hop virtual MIMO with collaborative beamforming

As shown in [22], the beampattern is only a relative measure of where the transmitted power is going. When compared with that, the antenna gain is the absolute measure of how much of the transmitted power is actually being transmitted in the direction ϕ, which can be obtained from the beampattern as

$$G(\phi/C_i) = \frac{2\pi P(\phi/C_i)}{\int_0^{2\pi} P(\theta/C_i)d\theta} \tag{3}$$

3.2. **Network communication model.** In this work, the multi-hop WSN is represented by the graph of $G = (V, E)$, wherein a vnode $i \in V$ denotes a cluster in the network, and a link $\{i, j\} \in E$ denotes the transmission that vnode i uses CB transmission to communicate with vnode j (or more precisely CH_j). In such a network, wireless communication can be modeled by the following equations commonly adopted in the literature:

$$P_{r_{\{i,j\}}} = \frac{P_{t_{\{i,j\}}} G_{t_{\{i,j\}}} G_{r_{\{i,j\}}}}{\gamma^{\kappa}_{\{i,j\}}} \left(\frac{\lambda}{4\pi}\right) \tag{4}$$

$$SINR_{\{i,j\}} = \frac{P_{r_{\{i,j\}}}}{\eta_j + \sum_{k \neq i,j} P_{r_{\{k,j\}}}} \tag{5}$$

$$LC_{\{i,j\}} = W \log_2(1 + SINR_{\{i,j\}}) \tag{6}$$

In the above, (4) denotes the receive power in j, wherein $P_{t_{\{i,j\}}}$ is the transmit power of i, $G_{t_{\{i,j\}}}$ is the corresponding transmit power gain, $G_{r_{\{i,j\}}}$ is the receive power gain, $\gamma_{\{i,j\}}$ is the Euclidean distance between i and j, and κ is the pathloss factor. Note that for CB, $G_{t_{\{i,j\}}}$ is obtained from (3) and is proportional to n_i^2 rather than n_i in the main lobe, as shown, for example, in [21], which reveals the reason why CB is considered more beneficial. Following that, (5) gives the SINR at receiver CH_j due to transmission from vnode i in the presence of other transmissions, wherein η_j is the thermal noise at CH_j. Finally, assuming that data is coded separately for each link and that the receiver considers unintended receptions as noises, (6) represents the channel capacity of WSN for a link $\{i, j\}$ according to the Shannon theory.

3.3. **Energy consumption model.** To model the energy consumption for the virtual MIMO with CB transmission (VMIMO-CB), instead of only considering the transmission energy consumption, we more precisely classify two components of energy consumption corresponding to the two phases in the communication: *Intracluster communication phase* and *Intercluster communication phase*.

- *Intracluster (ITA) communication phase*: During this phase, a cluster head, say CH_i, broadcasts the transmitted data to the other $n_i - 1$ member stations during time ς. The members in C_i except the head will receive and decode the data for cooperatively transmitting it to the next cluster head, say CH_j, afterward. For this phase, we have two energy components to be considered. The first component is due to power amplifier, and can be represented by

$$P_{pa_{local}} = (1 + \tau)P_{ts} \tag{7}$$

where τ is a factor associated with the drain efficiency of the power amplifier. The second component results from the other communication circuits, and can be obtained by

$$P_{CB_{local}} = P_{ct} + (n_i - 1)P_{cr} \tag{8}$$

In (8), P_{ct} denotes the energy consumption for the circuits on transmitting, and is approximated in [23] by $P_{DAC} + P_{mix} + P_{filt} + P_{syn}$, which involves the circuits on the transmitting mode: digital to analog converter (DAC), mixer (mix), active

filter at transmitter (*filt*) and frequency synthesizer (*syn*). Similarly, P_{cr} denotes the energy consumption for those on receiving, and can be approximated by $P_{LNA} + P_{mix} + P_{IFA} + P_{filr} + P_{ADC} + P_{syn}$, which involves the circuits on the receiving mode: low noise amplifier (*LNA*), intermediate frequency amplifier (*IFA*), active filter at receiver (*filr*) and analog to digital converter (ADC), in addition to *mix* and *syn*.

- *Intercluster (ITE) communication phase*: In this phase, n_i stations are arranged to jointly transmit data during time $1 - \varsigma$. That is, all stations in C_i will collaboratively contribute P_{tl} for such a transmission, and overall consume the energy for the amplifiers as

$$P_{pa_{long}} = (1 + \tau)P_{tl} \tag{9}$$

In addition, there are n_i stations in this phase to be the transmitters for a single receiver CH_j, which contributes the energy consumption

$$P_{CB_{long}} = n_i P_{ct} + P_{cr} \tag{10}$$

With the two phases, the energy consumption of vnode i for a link $\{i, j\}$ can be readily shown as

$$\widetilde{e_{\{i,j\}}} = \varsigma \left(P_{pa_{local}} + P_{CB_{local}}\right) + (1 - \varsigma) \left(P_{pa_{long}} + P_{CB_{long}}\right) \tag{11}$$

Similarly, the relay data rate for a link $\{i, j\}$ can be represented by

$$R_{b_{\{i,j\}}} = (1 - \varsigma)LC_{RE} \tag{12}$$

However, it has been indicated in [24] that the broadcast rate cannot be lower than the relay rate, i.e.,

$$\varsigma LC_{BC} \geq (1 - \varsigma)LC_{RE} \tag{13}$$

For the constraint of (13), we consider that in general cases for a useful VMIMO-CB application, wherein the distance $\gamma_{\{i,j\}}$ in ITE is much larger than that in ITA, the broadcast capacity LC_{BC} would be larger than the relay capacity LC_{RE}. Thus, as a simple strategy, letting $\varsigma = 1/2$ is adopted here to this end.

3.4. **Spatial-TDMA and scheduling.** As a scheduling-based MAC, time division multiple access (TDMA) can divide the spectral resources in an orthogonal manner by scheduling interfering links at different time slots, and would provide a better Qualify of Service (QoS) than its contention-based counterpart such as carrier sense multiple access (CSMA) did. Thus, in this work we consider a more general TDMA that can take into account the fact that in a wireless multi-hop network, if two links such that the transmitter of one link is separated by a large distance from the receiver of another link, and vice versa, then they would be scheduled simultaneously without inducing much interference. Based the concept, in [25], an variant of TDMA, namely Spatial-TDMA (STDMA), is introduced to furhter improve the efficiency of TDMA by allowing its time slots to be shared by simultaneously transmissions that are geographically separated. In addition, if each of wireless links supports a rate high enough, and the power consumption of transmission dominates the other energy consumptions in the system, then the simultaneous scheduling of weakly interfering links would lead to a reduction in the net power consumption. For these reasons, we adopt STDMA as the MAC protocol, and seamlessly integrate the SINR constraint into the scheduling. In order to represent its characteristics for the optimization, we have the following definitions.

Definition 3.1. *$\xi \subset E$ is a set of links that can be concurrently activated without violating the minimum SINR for communication, ζ. That is, all the receivers of the concurrent links in ξ must have their SINR values higher than ζ. If ξ can satisfy this constraint, it is called a transmission mode.*

Definition 3.2. *A scheduling matrix is defined as an indexed collection of transmission modes,* $\Xi = \{\xi_1, \ldots, \xi_k, \ldots, \xi_K\}$*, where* $K = |\Xi|$ *denotes the maximum index. A schedule* S *is called feasible if there exists a scheduling vector,* $\mathbf{p} = [p_1, \ldots, p_k, \ldots, p_K]$ *satisfying* $\sum_{1 \le k \le K} p_k \le 1$*, wherein* $p_k \ge 0$ *denotes the duration that all the links in* ξ_k *can be simultaneously active in the time frames of STDMA.*

4. Cross-Layer Approach for Network Lifetime Maximization.

4.1. The maximum lifetime cross-layer optimization problem (MLCLOP).

Taking into account the physical layer of VMIMO-CB and the MAC of STDMA, we can now formally consider the aim of this work: how to maximize the network lifetime of such WSNs with a cross-layer approach. Specifically, our aim here is to find the most energy-efficient scheduling that can maximize the network lifetime by jointly considering routing, scheduling and stream control problems for the WSNs operated under VMIMO-CB and STDMA. To this end, we consider 1) a rate allocation $\mathbf{r}$ specifying the rate r_m for each session m with source-destination pair, $\{s_m, d_m\}$, $1 \le m \le M$, to be the stream control variable, 2) a link allocation vector $\mathbf{f^m}$ specifying the amount of traffic $f^m_{\{i,j\}}$ of session m routed through link $\{i,j\}$ to be the routing variable, and 3) a transmission scheduling vector $\mathbf{p}$ specifying the time fraction p_k for each transmission mode ξ_k to be the scheduling variable. For the lifetime, we let each cluster or vnode, say $v \in V$, have an initial energy E_v uniformly distributed among its member stations. By means of these notations, the average energy per bit spent by vnode v for its outgoing link $\{i,j\}$ scheduled by $\mathbf{p}$ can be given by

$$\overline{e_{\{i,j\}}} = \frac{\sum_{k=1}^{K} p_k \widetilde{e_{\{i,j\}}}}{\sum_{k=1}^{K} p_k R_{b_{\{i,j\}}}} = \frac{\sum_{\forall \xi_k \in \Xi : \{i,j\} \in \xi_k} p_k \widetilde{e_{\{i,j\}}}}{\sum_{\forall \xi_k \in \Xi : \{i,j\} \in \xi_k} p_k R_{b_{\{i,j\}}}} \tag{14}$$

Then, by taking into account all the sessions $m \in M$ going through all the outgoing links $\{i,j\} \in E_v^{out}$, and the initial energy E_v, we have the lifetime for a vnode v in the network as

$$T_v = \frac{E_v}{\sum_{\{i,j\} \in E_v^{out}} \sum_{1 \le m \le M} \overline{e_{\{i,j\}}} f^m_{\{i,j\}}} \tag{15}$$

Given that, a well-known lifetime definition for WSN in the literature is considered here as the period from the start of network to the moment when the first vnode runs out of energy, i.e., $T = \min T_v$. With the above, we can formulate the maximum lifetime cross-layer optimization problem (**MLCLOP**) as

$$\begin{array}{lll}
\textbf{maximize} & T & (a) \\
\textbf{subject to} & \sum_{\{i,j\} \in E^{out}_{s_m}} f^m_{\{i,j\}} - \sum_{\{i,j\} \in E^{in}_{s_m}} f^m_{\{i,j\}} = r_m, \quad 1 \le m \le M & (b) \\
& \sum_{\{i,j\} \in E^{out}_{d_m}} f^m_{\{i,j\}} - \sum_{\{i,j\} \in E^{in}_{d_m}} f^m_{\{i,j\}} = -r_m, \quad 1 \le m \le M & (c) \\
(16) & \sum_{\{i,j\} \in E^{out}_{v}} f^m_{\{i,j\}} - \sum_{\{i,j\} \in E^{in}_{v}} f^m_{\{i,j\}} = 0, \quad 1 \le m \le M,\ \forall v \in V \backslash \{s_m, d_m\} & (d) \\
& \sum_{m=1}^{M} f^m_{\{i,j\}} \le \sum_{\forall \xi_k \in \Xi : \{i,j\} \in \xi_k} p_k \cdot R_{b_{\{i,j\}}}, \quad \forall \{i,j\} \in E & (e) \\
& T \sum_{\{i,j\} \in E^{out}_{v}} \sum_{1 \le m \le M} \overline{e_{\{i,j\}}} f^m_{\{i,j\}} \le E_v, \quad \forall v \in V & (f) \\
& \sum_{1 \le k \le K} p_k = 1 & (g) \\
& f^m_{\{i,j\}} \ge 0, \quad 1 \le m \le M,\ \forall \{i,j\} \in E & (h) \\
& p_k \ge 0, \quad 1 \le k \le K & (i) \\
& r_m \ge T L_m, \quad 1 \le m \le M & (j)
\end{array}$$

In the set of constraints, (16-b) represents the conservation law for source vnodes to ensure that the net amount of traffic going out of a session source is equal to its end-to-end session rate, and (16-c) symmetrically represents that for destination vnodes. (16-d) provides the conservation law for intermediate vnodes to ensure that the amount of traffic of a session entering any intermediate vnode is equal to that exiting the intermediate

vnode. In these constraints, $E^{out}_{s_m}/E^{out}_{d_m}/E^{out}_{v}$ ($E^{in}_{s_m}/E^{in}_{d_m}/E^{in}_{v}$) denotes the set of outgoing (incoming) links of source vnode s_m, destination vnode d_m, or the other vnode $v \in V$, respectively. (16-e) gives the bandwidth constraint to make sure that the total traffic on a link is no more than the average transmission rate. (16-f) denotes the lifetime constraint, showing that the lifetime of a vnode should be equal to or larger than the network lifetime. (16-g) gives the scheduling constraint, forcing that the summation of all elements in a transmission schedule vector is equal to 1. (16-h) and (16-i) simply represent the valid constraints for link rate and scheduling vector, respectively, and (16-j) gives the traffic load TL_m for each session m.

4.2. **Linear programming.** As can be seen readily, the MLCLOP formulation is not linear and may not be easily solved. More specifically, it poses the following challenges:

- The data rate $R_{b_{\{i,j\}}}$ in terms of link capacity $LC_{\{i,j\}}$ is a global function of all the interfering powers, and thus the transmit power is globally coupled with the other layers in the network.
- The variables of T, $\overline{e_{\{i,j\}}}$ (and thus p_k), and $f^m_{\{i,j\}}$ are nonlinearly coupled with each other in the constraint (16-f), which shows a complex relationship among the variables across the different layers.

To alleviate the first problem, the related works in [17, 18, 26] usually treat the power as a fixed value or formulate it as an variable to be solved for a real number solution that can reduce the computation complexity on finding the association between power and rate. Complementing these works, we introduce a column generation (CG) approach for the case of both power and rate being discrete to support the upper layers as the most practical scenario considered by the standards for implementation, which will be discussed in Section 6. For the second problem, we consider that if the transmission matrix Ξ is given a priori by the CG approach and so are $\widetilde{e_{\{i,j\}}}$ and $R_{b_{\{i,j\}}}$, a nonlinearity can be identified in the constraint (16-f) as the product of $T \times f^m_{\{i,j\}}$. For resolving the nonlinearity, a single variable $\widehat{f^m_{\{i,j\}}}$ is used to represents the total number of data for session m transmitted through link $\{i,j\}$ in the network lifetime T, rather than the product of these two variables. Similarly, p_k involved is replaced by $\widehat{p_k} = T \times p_k$ to denote the overall duration scheduled for transmission mode k in the network lifetime T. In addition, for the corresponding distributed algorithm to be presented, we consider to replace the hybrid representation of links and vnodes in (16) to be a node-centric representation that can focus on the relationship between a vnode i and its neighbors N_i. Taking these into account, we have

$$
\begin{array}{lllll}
\textbf{maximize} & T & & & (a)\\
\textbf{subject to} & \sum_{j\in N_i}\left(f^m_{\{i,j\}} - f^m_{\{j,i\}}\right) = R_{im}, & \forall i \in V, & 1 \le m \le M & (b)\\
& \sum_{1\le m\le M} \widehat{f^m_{\{i,j\}}} \le \sum_{\forall \xi_k \in \Xi:\{i,j\}\in\xi_k} \widehat{p_k} R_{b_{\{i,j\}}}, & \forall i \in V, & \forall j \in N_i & (c)\\
(17) & \sum_{j\in N_i}\sum_{1\le m\le M} \overline{e_{\{i,j\}}}\widehat{f^m_{\{i,j\}}} \le E_i, & \forall i \in V & & (d)\\
& \sum_{1\le k\le K} \widehat{p_k} = T & & & (e)\\
& f^m_{\{i,j\}} \ge 0, & \forall i \in V, & \forall j \in N_i, \quad 1 \le m \le M & (f)\\
& p_k \ge 0, & 1 \le k \le K & & (g)\\
& r_m \ge TL_m, & 1 \le m \le M & & (h)
\end{array}
$$

where

$$
R_{im} = \begin{cases} r_m, & \text{if } i \text{ is the source of session } m \\ -r_m, & \text{if } i \text{ is the sink of session } m \\ 0, & \text{otherwise} \end{cases} \tag{18}
$$

However, the above is still nonlinear. That is, it still exists the nonlinearity of $\sum_{j\in N_i}\sum_{1\le m\le M}\overline{e_{\{i,j\}}}\widehat{f^m_{\{i,j\}}} \le E_i$ in (17-d), which involves the products among the scheduling variables p_k and link allocation variables $f^m_{\{i,j\}}$. To resolve the nonlinearity, we multiply both sides of (17-c) with $\overline{e_{\{i,j\}}}$, leading to

$$\sum_{j\in N_i}\sum_{1\le m\le M}\overline{e_{\{i,j\}}}\widehat{f^m_{\{i,j\}}} \le \sum_{j\in N_i}\sum_{\forall \xi_k\in\Xi:\{i,j\}\in\xi_k}\overline{e_{\{i,j\}}}\widehat{p_k}R_{b_{\{i,j\}}}, \quad \forall i\in V \tag{19}$$

Then, by observing the relationship between (19) and (17-d) with $\overline{e_{\{i,j\}}}$ given in (14) and performing some algebra, we can find $\widehat{p_k}\widetilde{e_{\{i,j\}}}$ to replace $\overline{e_{\{i,j\}}}\widehat{f^m_{\{i,j\}}}$ in the above, which eventually leads to the following linear constraint

$$\sum_{j\in N_i}\sum_{\forall \xi_k\in\Xi:\{i,j\}\in\xi_k}\widehat{p_k}\widetilde{e_{\{i,j\}}} \le E_i, \quad \forall i\in V \tag{20}$$

Finally, the linear programming formulation for MLCLOP **(MLCLOP-LP)** can be represented as follows.

$$\textbf{maximize} \quad T \tag{21}$$

subjectto (b), (c), (e), (f), (g) and (h) of (17), while (d) of that is replaced by (20).

5. **Distributed Algorithm for MLCLOP (MLCLOP-DA).** In the previous section, we have introduced a linear programming formulation for MLCLOP. Obviously, it is a centralized algorithm to be useful when its parameters can be obtained appropriately. However, a distributed algorithm would be preferred when its centralized counterpart can not work efficiently for some reasons or the computation center would be a bottleneck of the network. Thus, to be a more complete work, we adopt the Lagrangian duality and a subgradient method for convex optimization to develop a distributed algorithm corresponding to MLCLOP-LP introduced above, as follows.

5.1. **Linear programming formulation for distributed algorithm.** To construct the distributed algorithm, we modify the formulation in (21) by changing the maximization of T to be the minimization of $q = 1/T$, resulting in an equivalent optimization. In addition, the changing variable of $\widehat{p_k} = T \times p_k$ in (17) and hence (21) is not required here because in (20) the involved T is moved to the right-hand side as q. By means of this, we can obtain another equivalent linear programming formulation as follows.

$$\begin{array}{lll}
\textbf{minimize} & q = 1/T & (a)\\
\textbf{subject to} & \sum_{j\in N_i}\left(f^m_{\{i,j\}} - f^m_{\{j,i\}}\right) = R_{im}, \quad \forall i\in V, \quad 1\le m\le M & (b)\\
& \sum_{1\le m\le M} f^m_{\{i,j\}} \le \sum_{\forall \xi_k\in\Xi:\{i,j\}\in\xi_k} p_k R_{b_{\{i,j\}}}, \quad \forall i\in V, \quad \forall j\in N_i & (c)\\
(22) & \sum_{j\in N_i}\sum_{\forall \xi_k\in\Xi:\{i,j\}\in\xi_k} p_k\widetilde{e_{\{i,j\}}} \le qE_i, \quad \forall i\in V & (d)\\
& \sum_{1\le k\le K} p_k = 1 & (e)\\
& f^m_{\{i,j\}} \ge 0, \quad \forall i\in V, \quad \forall j\in N_i, \quad 1\le m\le M & (f)\\
& p_k \ge 0, \quad 1\le k\le K & (g)\\
& r_m \ge TL_m, \quad 1\le m\le M & (h)
\end{array}$$

This results in a form that we will extend to solve in a distributed manner. However, it is still centralized because both q and p_k are global variables shared by all vnodes $i\in V$ and cannot be obtained by these vnodes independently. To be fully distributed, we let each vnode i have its own q_i and p_{ki}, and add the constraints (23-e) and (23-f) shown below that force all q_i and p_{ki} to be equal, respectively, for each vnode i. In addition, because

the object function minimizing q is equivalent to that minimizing $|V|\,q^2$ or $k_c\,q^2$, where $|V|$ is also denoted by k_c previously, and the object function of $|V|\,q^2$ is equal to that of $\sum_{\forall i\in V} q_i^2$ under the constraint just mentioned above, $q_i = q_j, \forall i,j \in V$. Consequently, MLCLOP can be reformulated as the following convex optimization problem:

$$
\begin{array}{lll}
\textbf{minimize} & q_i^2 & (a)\\
\textbf{subject to} & \sum_{j\in N_i}\left(f^m_{\{i,j\}} - f^m_{\{j,i\}}\right) = R_{im}, \quad \forall i\in V,\quad 1\le m\le M & (b)\\
& \sum_{1\le m\le M} f^m_{\{i,j\}} \le \sum_{\forall \xi_k\in\Xi:\{i,j\}\in\xi_k} p_{k\,i} R_{b_{\{i,j\}}}, \quad \forall i\in V,\quad \forall j\in N_i & (c)\\
& \sum_{j\in N_i}\sum_{\forall \xi_k\in\Xi:\{i,j\}\in\xi_k} p_{k\,i}\widetilde{e_{\{i,j\}}} \le q_i E_i, \quad \forall i\in V & (d)\\
(23) & q_i = q_j, \quad \forall i\in V,\quad \forall j\in N_i & (e)\\
& p_{k\,i} = p_{k\,j}, \quad \forall i\in V,\quad \forall j\in N_i,\ 1\le k\le K & (f)\\
& \sum_{1\le k\le K} p_{k\,i} = 1, \quad \forall i\in V & (g)\\
& f^m_{\{i,j\}} \ge 0, \quad \forall i\in V,\quad \forall j\in N_i,\ 1\le m\le M & (h)\\
& p_{k\,i} \ge 0, \quad \forall i\in V,\quad 1\le k\le K & (i)\\
& r_m \ge TL_m, \quad 1\le m\le M & (j)
\end{array}
$$

In what follows, we proceed to use the primal-dual approach to develop our distributed algorithm with the subgradient method. To this end, we note first that, apart from q_i, the objective function in (23) involves no $p_{k\,i}$ that are also distributed variables to be locally solved, and the sum of these variables (i.e., the scheduling length) would be simultaneously minimized by using its quadratic form ($p_{k\,i}^2$) along with the lifetime, for each vnode i. Besides, for each link allocation variable $f^m_{\{i,j\}}$, which can be decided independently by its definition, we also add a quadratic regularization term in the object function to eventually constitute a strict convex programming problem. When taking all the above into account and using σ to denote the regularization factor, we can approximate the optimization problem in (23) by

$$
\begin{array}{ll}
\textbf{minimize} & q_i^2 + \sum_{i\in V}\sum_{1\le k\le K} {p_{k\,i}}^2 + \sum_{i\in V}\sum_{j\in N_i}\sum_{1\le m\le M} \sigma {f^m_{\{i,j\}}}^2 \qquad (24)\\
\textbf{subject to} & \text{the same constraints of (23), while (g) of that is replaced by } \sum_{1\le k\le K} p_{k\,i} \le 1.
\end{array}
$$

5.1.1. *Dual problem.* To construct the dual problem, we introduce Lagrange multipliers α_{im} for the link conservation law, β_{ijk} for the equality constraint of scheduling, and γ_{ij} for the equality constraint of lifetime. Given that and the notations of $\hat{\mathbf{p}} = \left[\mathbf{p}_1, \mathbf{p}_2, \ldots, \mathbf{p}_{|V|}\right]$ wherein $\mathbf{p}_i = [p_{1\,i}, p_{2\,i}, \ldots, p_{K\,i}]$, and $\mathbf{q} = \left[q_1, q_2, \ldots, q_{|V|}\right]$ in addition to $\mathbf{f^m}$ introduced previously, we have the *Lagrangian*

$$
\begin{aligned}
& L\left(\mathbf{f^m}, \hat{\mathbf{p}}, \mathbf{q}, \alpha, \beta, \gamma\right) \qquad (25)\\
&= \sum_{i\in V} q_i^2 + \sum_{i\in V}\sum_{1\le k\le K} {p_{k\,i}}^2 + \sum_{i\in V}\sum_{j\in N_i}\sum_{1\le m\le M} \sigma {f^m_{\{i,j\}}}^2\\
&\quad + \sum_{i\in V}\sum_{1\le m\le M} \alpha_{im}\left\{\sum_{j\in N_i}\left(f^m_{\{i,j\}} - f^m_{\{j,i\}}\right) - R_{im}\right\}\\
&\quad + \sum_{i\in V}\sum_{j\in N_i}\sum_{1\le k\le K} \beta_{ijk}\left(p_{k\,i} - p_{k\,j}\right)\\
&\quad + \sum_{i\in V}\sum_{j\in N_i} \gamma_{ij}\left(q_i - q_j\right)
\end{aligned}
$$

$$= -\sum_{i\in V}\sum_{1\le m\le M}\alpha_{im}R_{im} + \sum_{i\in V} q_i^2 + \sum_{i\in V}\sum_{1\le k\le K} {p_{k\,i}}^2 + \sum_{i\in V}\sum_{j\in N_i}\left\{\sum_{1\le m\le M}\left(\sigma {f^m_{\{i,j\}}}^2 + f^m_{\{i,j\}}\left(\alpha_{im}-\alpha_{jm}\right)\right) + \sum_{1\le k\le K}\left(p_{k\,i}\left(\beta_{ijk}-\beta_{jik}\right)\right) + q_i\left(\gamma_{ij}-\gamma_{ji}\right)\right\}$$

Then, the dual function is given by

$$g(\alpha,\beta,\gamma) = \inf_{\mathbf{f^m}\succeq 0,\hat{\mathbf{p}}\succeq 0,\mathbf{q}\succeq 0}\left\{ L\left(\begin{array}{c}\mathbf{f^m},\hat{\mathbf{p}},\mathbf{q},\\ \alpha,\beta,\gamma\end{array}\right) \;\middle|\; \begin{array}{l} \sum_{j\in N_i}\sum_{1\le m\le M} f^m_{\{i,j\}} \\ \le \sum_{j\in N_i}\sum_{\forall\xi_k\in\Xi:\{i,j\}\in\xi_k} p_{k\,i}R_{b_{\{i,j\}}},\ \forall i\in V,\ \forall j\in N_i \\ \sum_{j\in N_i}\sum_{\forall\xi_k\in\Xi:\{i,j\}\in\xi_k} p_{k\,i}\widetilde{e_{\{i,j\}}} \le q_iE_i,\ \forall i\in V \\ \sum_{1\le k\le K} p_{k\,i}\le 1,\ \forall i\in V \\ f^m_{\{i,j\}}\ge 0,\ \forall i\in V,\forall j\in N_i, 1\le m\le M \\ p_{k\,i}\ge 0,\ \forall i\in V, 1\le k\le K \\ r_m\ge TL_m,\ 1\le m\le M \end{array}\right\}$$

$$= -\sum_{i\in V}\sum_{1\le m\le M}\alpha_{im}R_{im} + \sum_{i\in V}\inf_{\substack{\mathbf{f^m}\succeq 0,\hat{\mathbf{p}}\succeq 0,\mathbf{q}\succeq 0,\\ j\in N_i,1\le k\le K,1\le m\le M}}\left\{ q_i^2 + \sum_{1\le k\le K} {p_{k\,i}}^2 + \sum_{j\in N_i}\left\{\sum_{1\le m\le M}\left(\sigma {f^m_{\{i,j\}}}^2 + f^m_{\{i,j\}}\left(\alpha_{im}-\alpha_{jm}\right)\right) + \sum_{1\le k\le K}\left(p_{k\,i}\left(\beta_{ijk}-\beta_{jik}\right)\right) + q_i\left(\gamma_{ij}-\gamma_{ji}\right)\right\} \;\middle|\; \sum_{j\in N_i}\sum_{1\le m\le M} f^m_{\{i,j\}} \le \sum_{j\in N_i}\sum_{\forall\xi_k\in\Xi:\{i,j\}\in\xi_k} p_kR_{b_{\{i,j\}}},\ \sum_{j\in N_i}\sum_{\forall\xi_k\in\Xi:\{i,j\}\in\xi_k} p_k\widetilde{e_{\{i,j\}}} \le q_iE_i,\ \sum_{1\le k\le K} p_{k\,i}\le 1,\ f^m_{\{i,j\}}\ge 0,\ p_{k\,i}\ge 0,\ r_m\ge TL_m\right\} \tag{26}$$

Note that, starting with (23) we have reformulated the global variables q and p_k in the network to be their distributed counterparts q_i and $p_{k\,i}$ that are local to each vnode $i\in V$, as shown in the above. Thus, it can be readily seen that the dual function derived can be evaluated separately in the local variables given in $\mathbf{f^m}$, $\hat{\mathbf{p}}$ and $\mathbf{q}$. Assume that there always exists feasible sessions satisfying the link conservation law (23-b), the bandwidth or rate scheduling constraint (23-c), the equality constraint of lifetime (23-e), and the equality constraint of scheduling (23-f). In addition, the energy conservation law (23-d) can be easily done by choosing a large enough value of q_i. Then the problem can satisfy the Slater's condition and hence the strong duality holds. That is, it is feasible to apply the primal-dual approach for the optimization. Finally, we adopt the subgradient method to complete our distributed algorithm as follows.

5.1.2. *Subgradient-based distributed algorithm.* Derived from the dual function (26), we can now formulate the subgradient-based distributed algorithm operated in an iterative manner. Specifically, in each iteration k, each vnode $i\in V$ will solve the following convex

programming with variables $f^m_{\{i,j\}}$, $p_{k\,i}$ and q_i.

$$
\begin{array}{lll}
 & q_i^2 + \sum_{1\le k\le K} {p_{k\,i}}^2 & \\
\textbf{minimize} & + \sum_{j\in N_i} \left\{ \sum_{1\le m\le M} \left(\sigma {f^m_{\{i,j\}}}^2 + f^m_{\{i,j\}} \left(\alpha^{(k)}_{im} - \alpha^{(k)}_{jm} \right) \right) \right. & (a) \\
 & \left. + \sum_{1\le k\le K} \left(p_{k\,i} \left(\beta^{(k)}_{ijk} - \beta^{(k)}_{jik} \right) \right) + q_i \left(\gamma^{(k)}_{ij} - \gamma^{(k)}_{ji} \right) \right\} & \\
\textbf{subject to} & \sum_{1\le m\le M} f^m_{\{i,j\}} & \\
 & \le \sum_{\forall \xi_k \in \Xi : \{i,j\}\in\xi_k} p_{k\,i} \widetilde{R_{b_{\{i,j\}}}}, & \forall j \in N_i \quad (b) \\
 & \sum_{j\in N_i} \sum_{\forall \xi_k \in \Xi : \{i,j\}\in\xi_k} p_{k\,i} \widetilde{e_{\{i,j\}}} \le q_i E_i, & (c) \\
 & \sum_{1\le k\le K} p_{k\,i} \le 1, & (d) \\
(27) & f^m_{\{i,j\}} \ge 0, & \forall j \in N_i, \quad 1 \le m \le M \quad (e) \\
 & p_{k\,i} \ge 0, & 1 \le k \le K \quad (f) \\
 & r_m \ge T L_m, & 1 \le m \le M \quad (g)
\end{array}
$$

Once obtaining the optimal values in iteration k, say ${f^m_{\{i,j\}}}^{(k)}$, ${p_{k\,i}}^{(k)}$ and $q_i^{(k)}$ from the convex programming, each vnode i can then compute the subgradient of $-g$ at $\left(\alpha^{(k)}_{im}, \beta^{(k)}_{ijk}, \gamma^{(k)}_{ij}\right)$ by

$$
\begin{cases}
f^{(k)}_{\alpha} = R_{im} - \sum_{j\in N_i} \left({f^m_{\{i,j\}}}^{(k)} - {f^m_{\{j,i\}}}^{(k)} \right) \\
f^{(k)}_{\beta} = {p_{k\,j}}^{(k)} - {p_{k\,i}}^{(k)} \\
f^{(k)}_{\gamma} = q_j^{(k)} - q_i^{(k)}
\end{cases}
\tag{28}
$$

With these results, it can further obtain the Lagrange multipliers for the next iteration $(k+1)$ by

$$
\begin{cases}
\alpha^{(k+1)}_{im} = \alpha^{(k)}_{im} - \delta_k f^{(k)}_{\alpha}, & 1 \le m \le M \\
\beta^{(k+1)}_{ijk} = \beta^{(k)}_{ijk} - \delta_k f^{(k)}_{\beta}, & \forall j \in N_i, \ 1 \le k \le K \\
\gamma^{(k+1)}_{ij} = \gamma^{(k)}_{ij} - \delta_k f^{(k)}_{\gamma}, & \forall j \in N_i
\end{cases}
\tag{29}
$$

It is evident that the algorithm shown in above is fully distributed. That is, each vnode can compute its primal variables (i.e., $f^m_{\{i,j\}}$, $p_{k\,i}$ and q_i) by itself, using the dual variables (i.e., the Lagrange multiplier α_{im}, β_{ijk} and γ_{ij}) of itself and its neighboring vnodes. In this process, the computations in (28) and (29) involve only evaluating linear functions, needing very low computation powers. In addition, the message exchange is limited within one-hop neighbors, which greatly reduces the communication overheads.

6. **Column Generation for MLCLOP (MLCLOP-CG).** In spite of the subgradient-based distributed algorithm, which involves the convex programming, MLCLOP itself is reformulated in Section 4.2 as a linear programming problem and its complexity lies in the computation of the set of all transmission modes. In fact, similar to that in [14] showing exponential time complexity for their link scheduling problem, we have here $K = 2^{|E|}$ transmission modes to be enumerated for the optimal solution, which is not computationally efficient and should be solved with a method that can avoid the explicit enumeration. In particular, the cross-layer formulation involves not only scheduling and power control but also routing and link control, which is a more complete or more complex cross-layer approach than that involving only part of them. Given the complexity, evaluating all possible transmission modes for a non-trial WSN to obtain its maximum network lifetime with a single computation is almost impossible. Thus, to incrementally improve the lifetime, we adopt here a *column generation* (CG) approach that decomposes the optimization problem into a *master problem* that involves the MLCLOP optimization

introduced above and a *sub-problem* that represents a systematical approach for adding a transmission mode under the transmission constraints based on SINR values.

More precisely, we conduct the master problem as a restricted version of MLCLOP, which considers only a subset of available columns or transmission modes, rather than $2^{|E|}$ such modes in total. That is, it uses only a sub-matrix $\Xi^o \subset \Xi$ with its index $K^o \leq K$ for this problem, and can be formulated as

$$[\textbf{MASTER}] : \textbf{maximize} \quad T \tag{30}$$
$$\textbf{subject to} \quad \text{the same constraints of (22), with } \Xi \text{ now replaced by } \Xi^o.$$

6.1. **Sub-problem.** Given the master problem, we now need to identify whether its result can be re-optimized by adding a new transmission mode to Ξ^o. Denoting the dual variables corresponding to constraint (22-c) by $w_{\{i,j\}}$, we suggest to find a transmission mode ξ_k that can maximize $\sum_{\{i,j\}\in E} w_{\{i,j\}} R_{b_{\{i,j\}}} \frac{E_i}{\widetilde{e_{\{i,j\}}}}$. The object function is so conducted because $\frac{E_i}{\widetilde{e_{\{i,j\}}}}$ readily represents the lifetime of a link $\{i,j\}$, and the relay rate $R_{b_{\{i,j\}}}$ would contribute an valid constraint for the session traffic on a link $\{i,j\}$ when maximizing the lifetime. Obviously, the object function is nonlinear. To linearize it, we simplify this function by considering that the local transmit power, P_{ts}, can be a fixed value sufficient for the ITA broadcast, and, $n_i, \forall i$, can be chosen a priori. Then, the transmit power for the relay transmission, P_{tl}, involved in the second term of (11) would be the variable for power adaptation. Hence, we can approximate $\widetilde{e_{\{i,j\}}}$ by P_{tl}, leading to the following maximization problem

$$\max \left(\sum_{\{i,j\}\in E} \frac{w_{\{i,j\}} R_{b_{\{i,j\}}} E_i}{P_{tl}} \right) \tag{31}$$

However, the problem shown in above is still non-linear. Fortunately, we can use a logarithmic transformation to reformulate it as a more tractable and equivalent linear problem as follows:

$$\max \left(\sum_{\{i,j\}\in E} \log(w_{\{i,j\}}) + \log(R_{b_{\{i,j\}}}) + \log(E_i) - \log(P_{tl}) \right) \tag{32}$$

6.2. **Power and rate adaptation scheme.** Note that finding a new column or transmission mode for MLCLOP depends on the power and rate adaptation schemes to be employed and the restrictions on the VMIMO-CB medium access. Thus, in the cross-layer optimization, we should consider how to formulate the power and rate adaption schemes for the sub-problem to comply with these constraints. For this issue, we notice that there are different power and rate transmission schemes being proposed in the literature, ranging from fixed power fixed rate (FPFR) to variable power variable rate (VPVR). For example, a FPFR scheme has been considered for STDMA in [27] due to its simplicity. However, by fixing the data rate, the system can not gain any additional link capacity even if its SINR values on some links remarkably exceed ζ, which obviously wastes the energies. In addition, the maximum power used can result in higher interference, leading to a smaller number of links to be concurrently activated. For solving these drawbacks, the research works, e.g., [13, 16, 18], naturally go toward variable power and/or rate transmission schemes.

Nevertheless, allowing a wireless sensor station to transmit with arbitrary power and to conduct arbitrary data rate is impractical for implementation. In fact, a realistic physical design for WSNs, e.g., the IEEE 802.15.4 compliant transceiver examined in [28], can support only several (8 in [28]) radio modes, and each mode is associated with a discrete

transmit power. Hence, it is more proper to consider that each vnode in the network supports only a number of power levels. That is, a link $\{i,j\}$ is only allowed to be active with a power level $P^{\hat{p}} \in \{P^1, P^2, \ldots, P^{\hat{p}_{\max}}\}$. Similarly, it is only allowed to transmit with a relay rate level $R^{\hat{r}} \in \{R^1, R^2, \ldots, R^{\hat{r}_{\max}}\}$. To this end, we introduce Boolean variable $y^{\hat{p}}_{\{i,j\}}$ for the relay transmit power of a link $\{i,j\}$, having its value of 1 if it transmits at the power level of $\hat{p}$, and 0 otherwise. Similarly, we introduce Boolean variable $x^{\hat{r}}_{\{i,j\}}$ for the relay rate of a link $\{i,j\}$, having its value of 1 if it transmits at the relay rate level of $\hat{r}$, and 0 otherwise. With these variables, the discrete power and discrete rate (DPDR) transmission scheme can be formulated as the following binary integer programming problem.

$$\textbf{[Sub-DPDR]} \quad \max \left(\sum_{\{i,j\}\in E} \left(\sum_{\hat{r}=1}^{\hat{r}_{\max}} \left(\log(w_{\{i,j\}}) + \log(R^{\hat{r}}) + \log(E_i) \right) x^{\hat{r}}_{\{i,j\}} - \sum_{\hat{p}=1}^{\hat{p}_{\max}} \log(P^{\hat{p}}) y^{\hat{p}}_{\{i,j\}} \right) \right) \tag{a}$$

$$\textbf{subject to} \quad \zeta_{\hat{r}} \left(\eta_j + \sum_{a\neq i,j} P^{\max}_{r_{\{a,j\}}} \right) x^{\hat{r}}_{\{i,j\}} + \zeta_{\hat{r}} \sum_{a\neq i,j} \sum_{\hat{p}=1}^{\hat{p}_{\max}} P^{\hat{p}}_{r_{\{a,j\}}} - \sum_{\hat{p}=1}^{\hat{p}_{\max}} P^{\hat{p}}_{r_{\{i,j\}}}$$

$$\leq \zeta_{\hat{r}} \sum_{a\neq i,j} P^{\max}_{r_{\{a,j\}}}, \qquad \forall \{i,j\} \in E, \quad 1 \leq \hat{r} \leq \hat{r}_{\max} \tag{b}$$

$$\sum_{j:\{i,j\}\in E} x^{\hat{r}}_{\{i,j\}} + \sum_{j:\{j,i\}\in E} x^{\hat{r}}_{\{j,i\}} \leq 1, \quad \forall i \in V, \qquad 1 \leq \hat{r} \leq \hat{r}_{\max} \tag{c}$$

$$\sum_{\hat{r}=1}^{\hat{r}_{\max}} x^{\hat{r}}_{\{i,j\}} \leq 1, \qquad \forall \{i,j\} \in E \tag{d}$$

$$\sum_{\hat{p}=1}^{\hat{p}_{\max}} y^{\hat{p}}_{\{i,j\}} \leq 1, \qquad \forall \{i,j\} \in E \tag{e}$$

$$x^{\hat{r}}_{\{i,j\}} \in \{0,1\}, \qquad \forall \{i,j\} \in E, \quad 1 \leq \hat{r} \leq \hat{r}_{\max} \tag{f}$$

$$y^{\hat{p}}_{\{i,j\}} \in \{0,1\}, \qquad \forall \{i,j\} \in E, \quad 1 \leq \hat{p} \leq \hat{p}_{\max} \tag{g}$$

(33)

In the formulation, we note two conditions to be satisfied for the VMIMO-CB network. The first is called *valid transmission*, which corresponds to the contention constraint shown in (33-c) enforcing that a node can not send and receive at the same time due to the half duplex nature of a sensor station adopted. The second is called *admissible transmission*, denoting that there is an admissible set of vnodes that can safely transmit in a slot without disrupting each other's transmission. Here, it corresponds to the SINR constraint given in (33-b) showing that if link $\{i,j\}$ is selected, its SINR value should be larger than or equal to $\zeta_{\hat{r}}$ to conduct an admissible transmission on this link, whereas if $\{i,j\}$ is not selected, the result is at least an valid constraint for the system. Therein $\zeta_{\hat{r}}$ is the SINR requirement for a discrete rate level of $\hat{r}$, and $P^{\hat{p}}_{r_{\{x,y\}}}$ is the receive power for vnode y when vnode x uses a discrete power level of $\hat{p}$ to transmit its data. Apart from the above, (33-d) gives the constraint that each link can transmit at most a single rate if it is activated, and (33-e) is used to allow a link to transmit with only one power level. Finally, (33-f) and (33-g) involved simply denote the discrete nature of its rate and that of its power (represented by the corresponding Boolean variables), respectively.

7. **Experiment Results.** In this section, we report on numerical results for the optimization schemes introduced previously. Specially, we conduct simulation experiments with a regular network topology to examine the cross-layer optimization MLCLOP-CG, and conduct the experiments with a random topology to verify the distributed algorithm MLCLOP-DA.

7.1. **Regular topology (for MLCLOP-CG).** As abstractly represented in Figure 2(a), we simulate a network of $N = 1200$ sensor stations that are divided into $k_c = 9$ clusters or vnodes; each of them has $M_i \approx 133$ stations randomly distributed over an rectangle area of $2u \times 2u$, where u denotes the wavelength of carrier to be considered. Furthermore, each vnode i selects $n_i = |C_i| = 100$ stations for communication and selects the station

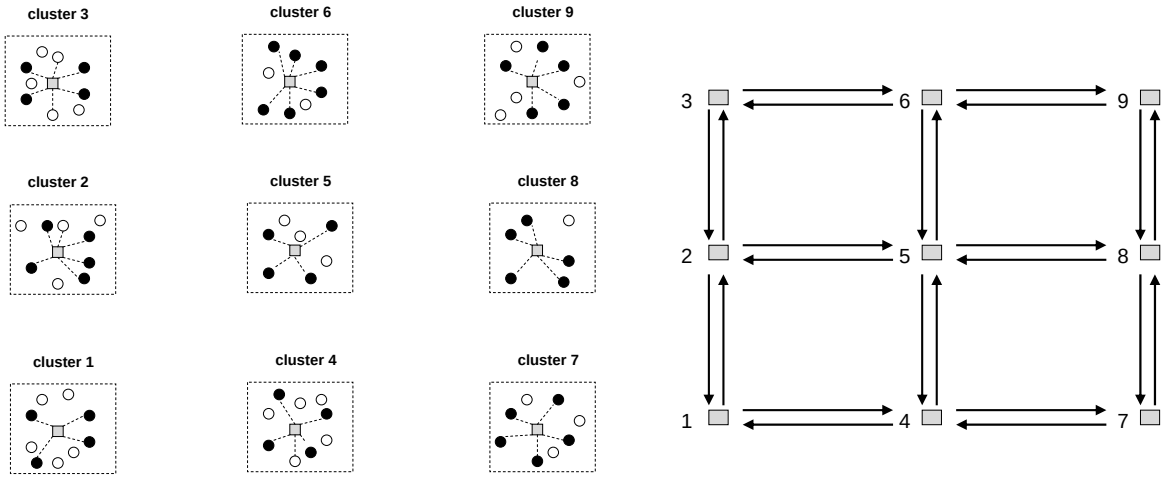

FIGURE 2. Regular experimental topology: (a) an abstract expression of the cluster or vnode graph, and (b) its initial set of links

TABLE 1. System parameters for the experiments

Symbol	Quantity	Symbol	Quantity
P_{mix}	30.3 mW [23]	P_{syn}	50 mW [23]
P_{flit}	2.5 mW [23]	P_{flir}	2.5 mW [23]
P_{ADC}	9.85 mW [23]	P_{DAC}	15.48 mW [23]
P_{LNA}	20 mW [23]	P_{IFA}	3 mW [23]
W	250 KHz	α	2 : local, 3 : long-haul
$\zeta_{\hat{r}}$	$2^{R^{\hat{r}}/W} - 1$	β	1.9 [29]
$P^{\hat{p}}$, $R^{\hat{r}}$, $R_{b_{local}}$	shown in Table 3	η	10^{-10}

TABLE 2. Radio modes and their power consumptions for P_t (P_{ts}, P_{tl}) (quoted from [28])

Radio mode	Power Consumption	Radio Mode	Power Consumption
TX_1 (–25 dBm)	26.6 mW	TX_2 (–15 dBm)	29.8 mW
TX_3 (–10 dBm)	32.9 mW	TX_4 (–7 dBm)	36.0 mW
TX_5 (–5 dBm)	39.1 mW	TX_6 (–3 dBm)	42.1 mW
TX_7 (–1 dBm)	45.0 mW	TX_8 (0 dBm)	48.0 mW

closest to the centre as its cluster head, CH_i. Specifically, we conduct the topology so that the distance between two horizontally (vertically) neighboring vnode centres is $200u$, resulting in a regular topology that can simply exhibit the experiment results in details. In addition, we let P_{ts} be TX_1, which would be sufficient for the intra-cluster communication, and P_{tl} be TX_2 for the initial set of links but afterward it (P_{tl}) can be any transmission mode in Table 2 for the CG approach. Apart from the above, the other parameters for the power efficiency calculation, including circuit parameters and system parameters, are summarized in Table 1, and those specific to the different experiment sets are given in Table 3.

TABLE 3. Experiment sets

Tag	Relay Transmit Power Set $\{P^{\hat{p}}\}$	Relay Rate Set $\{R^{\hat{r}}\}$
1 (4 powers)	$\{TX_1, TX_2, TX_3, TX_4\}$	$\begin{cases} \{\frac{1}{8}R^M, \frac{2}{8}R^M, \frac{3}{8}R^M, \frac{4}{8}R^M\}, \\ \{\frac{1}{8}R^M, \frac{2}{8}R^M, \frac{3}{8}R^M, \frac{4}{8}R^M, \frac{5}{8}R^M, \frac{6}{8}R^M, \frac{7}{8}R^M, R^M\} \end{cases}$
2 (8 powers)	$\{TX_1, TX_2, TX_3, TX_4,$ $TX_5, TX_6, TX_7, TX_8\}$	$\begin{cases} \{\frac{1}{8}R^M, \frac{2}{8}R^M, \frac{3}{8}R^M, \frac{4}{8}R^M\}, \\ \{\frac{1}{8}R^M, \frac{2}{8}R^M, \frac{3}{8}R^M, \frac{4}{8}R^M, \frac{5}{8}R^M, \frac{6}{8}R^M, \frac{7}{8}R^M, R^M\} \end{cases}$

At the beginning of a simulation, we set an initial Ξ^o composed of ξ_i, $1 \le i \le K^o = 24$, as shown in Figure 2(b), and each transmission mode ξ_i contains only a single link that is established by a sufficient power level, TX_2, for the relay transmission. Given that, we conduct three sessions, $\{s_1 = 1, d_1 = 9\}$, $\{s_2 = 2, d_2 = 9\}$ and $\{s_3 = 4, d_3 = 9\}$ with their traffic loads $TL \approx 22.56$ Kbps as the session rates to be satisfied in the MLCLOP optimization. With the few sections, we can clearly observe the behaviors of the cross-layer optimization, instead of manipulating many sections with randomly deployed source-destination pairs that may disturb the viewpoint. In fact, as shown in [16], even an approach along with a continuous power adaptation would have exponential time complexity in the number of communication links, and computing exact solutions is, in general, NP-hard. Here, in addition to the number of links, our MLCLOP-CG should also take into account the discrete power and discrete rate adaptation, inevitably resulting in a more complex integer programming problem of Sub-DPDR. Moreover, since we do not consider any restriction on $SINR_{\{i,j\}}$ for the link capacity, the topology resulted actually corresponds to a fully connected network. Thus, for computation efficiency, we demonstrate here at most eight power levels and eight data rates that are widely considered in the standards such as IEEE 802.11a [30] and IEEE 802.15.4 [31]. This already yields $72 \times 8 \times 2 = 1152$ binary integer variables for the experiments and actually consumes a lot of computation time for a limited number of CG iterations.

Now two different sets for the experiments are so arranged by the combination of 4 and 8 power levels of P_{tl} with 4 and 8 transmit data rates of R_b, as shown in Table 3. In this table, $R^M \approx 1.386$ Mbps is given by 0.8 times the maximum relay data rate obtainable in the network. Given that, 100 iterations of the column generation (CG) in Section 6 are carried out for all the experiment instances. In addition to the proposed methods, we examine also a TDMA-based optimization scheme, namely TDMA-LP, wherein a transmission mode contains only a single link in the network, and every $P^{\hat{p}}$ is evaluated on each link $\{i, j\}$ for obtaining all possible $R^{\hat{r}}$'s in the latter. Obviously, TDMA-LP represents the optimal method in TDMA to compare with our methods in STDMA within a reasonable time constraint. Figure 3 shows the optimization results for the different methods, where (a) exhibits the results of 4 powers and 4 rates, (b) shows that of 4 powers and 8 rates, and similarly, (c) and (d) demonstrate the results of 8 powers along with 4 rates and 8 rates, respectively. In each subgraph, the top half exhibits the results of MLCLOP-CG and the bottom half shows those of TDMA-LP, and in the third of each, the thickness of an arrow-line is used to represent its value of link allocation resulted from the corresponding optimization. From this figure, we have the following observations. First, due to the limited number of iterations, MLCLOP-CG has its performance results slightly different from those of TDMA-LP. However, the trend of these results is the same. For example, given 4 powers and 4 rates, Figure 3(a) shows that both MLCLOP-CG and TDMA-LP tend to enjoy the highest rate (rate 4) with the powers large enough (power 3 and power 4). As another example, when the rate level increases to 8 and the power level remains 4, Figure 3(b) shows that both methods would more aggressively use the

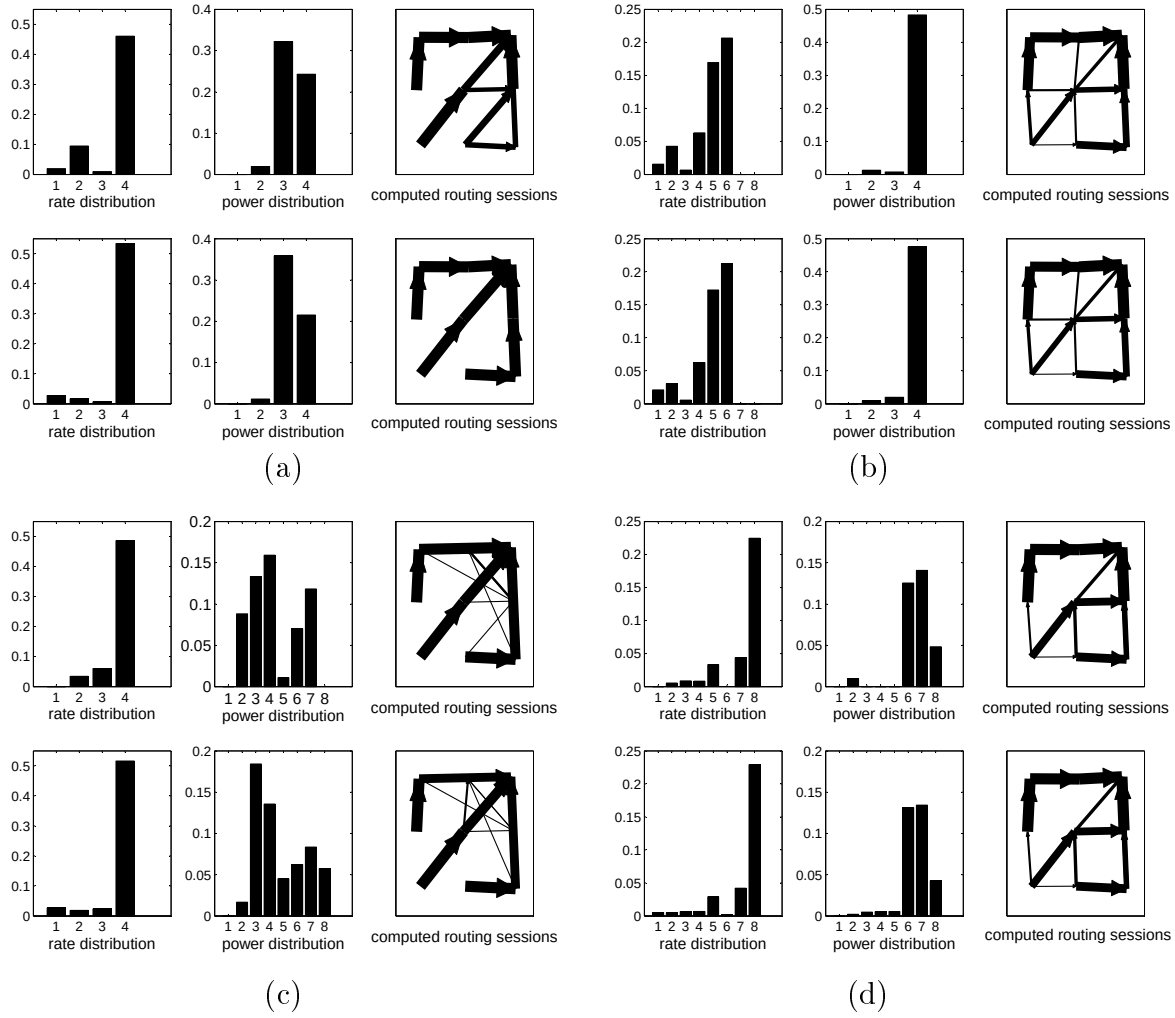

FIGURE 3. Results of MLCLOP-CG and TDMA-LP: (a) 4 powers and 4 rates, (b) 4 powers and 8 rate, (c) 8 powers and 4 rates, and (d) 8 powers and 8 rates. In each subgraph, the top (bottom) half exhibits the results of MLCLOP-CG (TDMA-LP).

highest power to obtain the higher data rates offerable (rate 6) for achieving even better energy-efficient transmission and prolonging the network lifetime. Second, we observe that when the number of rates is limited to 4, despite the number of rates (4 or 8), the computed routing links for session $\{s_m = 1, d_m = 9\}$ tend to follow the shortest path, i.e., $1 \to 5 \to 9$, with only certain traffic split toward the other vnodes, as shown in Figures 3(a) and 3(c). However, as shown in Figures 3(b) and 3(d), when the number of rates increases to 8, the traffic for this session would contribute more to the vnodes not in the shortest path, resulting in the more energy-efficient transmissions for the lifetime.

The third and final point worth noting is that even though MLCLOP-CG and TDMA-LP have slight differences on the power/rate/link allocations, their lifetimes are almost identical, as shown in Figure 4. In this figure, we can see also that due to the same initial setting, the lifetimes obtained by solving the master problem (30) at the first time for the four experiment sets are the same, as expected. As expected also, increasing the number of rates will increase the energy-efficiency and hence improves the lifetime. However, it is worth noting that as the number of rates remains 4 in the experiment, increasing the number of powers from 4 to 8 can hardly increase the lifetime. That is to say, when

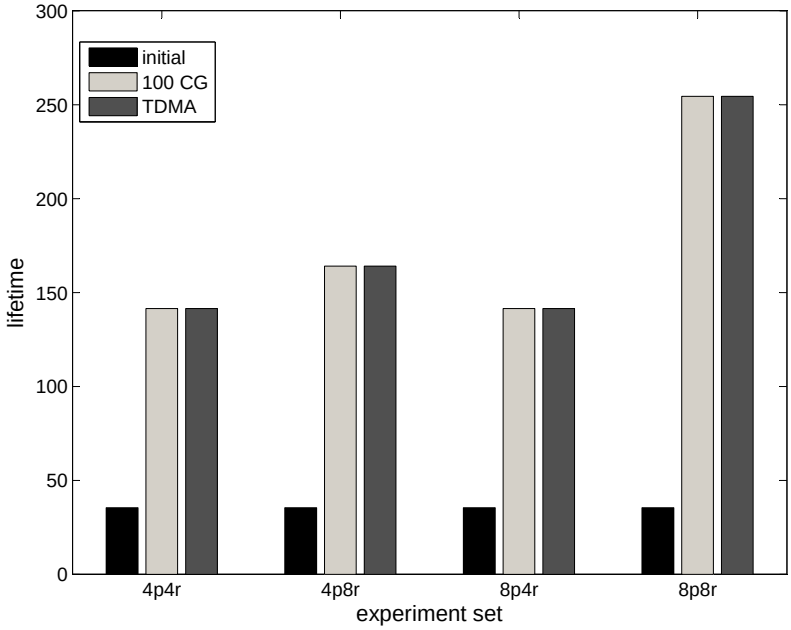

FIGURE 4. Energy consumption results for different combinations of powers and rates

simply increasing the transmit power without correspondingly increasing the data rate, the energy consumption per bit for a link is not improved and the lifetime is not increased as a result.

7.2. **Random topology (for MLCLOP-DA).** In the set of experiments, we conduct a random topology shown in Figure 5(a) as the simulation environment, wherein 9 vnodes with their centres are located in a $400u \times 400u$ square area, and each vnode i has $70 \leq |M_i| = |C_i| \leq 100$ stations randomly distributed over a $2u \times 2u$ square area around its centre. The parameters for the energy consumption model are the same as those for the regular topology summarized in Table 1. However, since no CG to be involved, this random topology shown in Figure 5(a) is a complete connectivity graph, whereas the regular counterpart shown in Figure 2(b) is just its initial set of links. Given that, we conduct six sessions, $\{s_1 = 4, d_1 = 3\}$, $\{s_2 = 1, d_2 = 6\}$, $\{s_3 = 3, d_3 = 4\}$, $\{s_4 = 6, d_4 = 1\}$, $\{s_5 = 8, d_5 = 7\}$ and $\{s_6 = 7, d_6 = 8\}$, and each session imposes its traffic load of $TL = 2$ Kbps on the MLCLOP optimization. In addition, we adopt $P^2 = TX_2$ as the transmit power that is high enough to support the minimum data rate (R^1) for each link, and equip each vnode i with the same amount of E_i to avoid the bias upon those with weak initial energies.

With the random topology given in Figure 5(a), the corresponding results for the experiment are shown in Figures 5(b)-5(d), respectively. In Figure 5(b), the computed routing links for the six sessions are shown by the lines with different thickness to relatively represent the link allocations resulted from MLCLOP-DA. Clearly, we can see that the links between vnode 2 and vnode 7 have the maximal values because all the traffic must go through them. Moreover, we can also see that due to the nature of lifetime maximization, the computed routing links are more possibly distributed to different edges to result in more energy-efficient communications for an increased lifetime, when compared with a minimum energy optimization counterpart that would focus on the most energy-efficient paths and hence shorten the lifetime as a result of its ignorance of E_i.

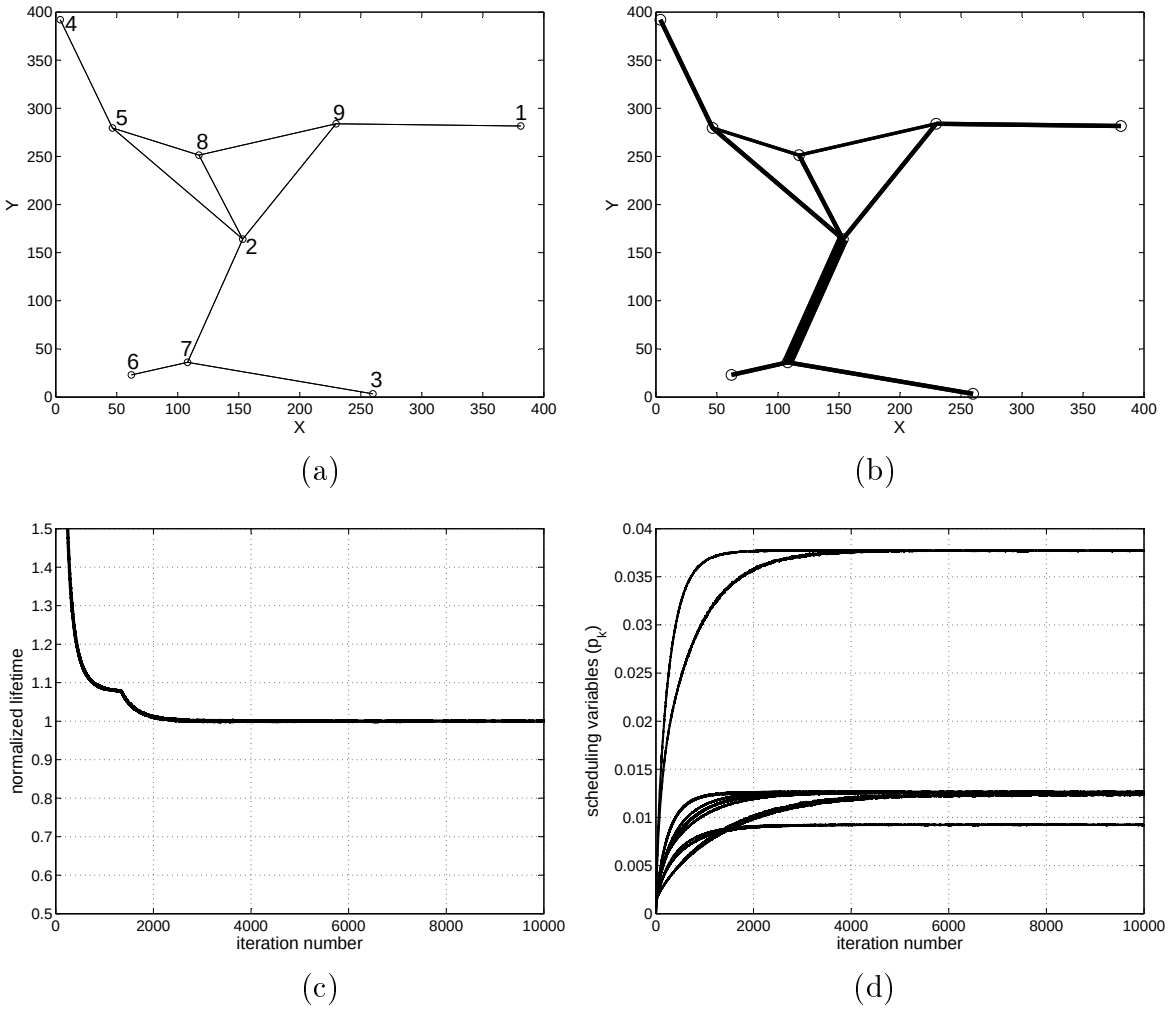

FIGURE 5. Results of MLCLOP-DA: (a) connectivity graph for the random topology, (b) computed routing links for the sessions, (c) normalized lifetime, and (d) scheduling variables

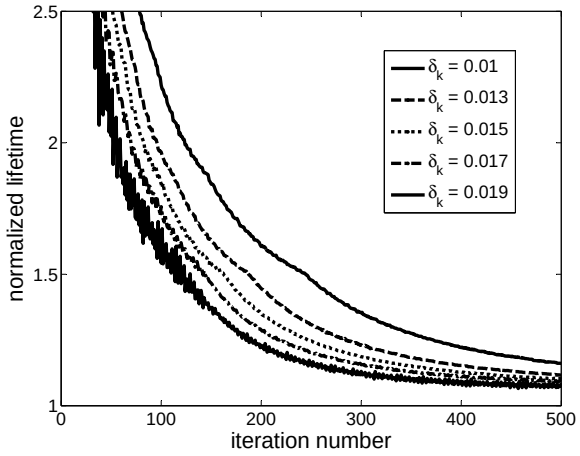

FIGURE 6. Comparison results on different δ_k

In Figure 5(c), the normalized lifetime is given by $\frac{T_{mlclop-da}}{T_{mlclop-lp}}$, where $T_{mlclop\text{-}da}$ denotes the lifetime obtained by the distributed algorithm MLCLOP-DA, and $T_{mlclop\text{-}lp}$ denotes

that by the linear programming MLCLOP-LP given in (22). As can be seen readily, the normalized lifetime converges to 1 after 2K CG iterations in the experiment. That is, the distributed version can achieve the same lifetime as the centralized counterpart did if given enough CG iterations. Besides, the other distributed variables to be optimized, i.e., the scheduling variables, p_k, $1 \leq k \leq K = 20$, are given in Figure 5(d). From this figure, we can see these variables actually converging to about three quantities after 4K CG iterations. Note that, apart from the lifetime itself, the many scheduling variables to be concurrently converged indeed increase the time complexity. However, it should be also noted that although the number of iterations seems to be high in the instance, it is just used to demonstrate how much a rigor requirement on convergence can achieve. In fact, as shown in Figure 5(c), given $\delta_k = 0.01$, the normalized lifetimes can fast converge on 1.16 with only 500 iterations which is a number fairly far from the end of this experiment. To confirm the trend of convergence, we conduct another set of experiments by varying the step size δ_k from 0.013 to 0.019 under the same 500 iterations, in addition to that of 0.01 which is also included here to represent the baseline for comparison. Their results of the average lifetimes are now depicted in Figure 6. From this figure, it can be seen that as δ_k slightly increases from 0.01 to 0.019, the lifetimes converge faster from 1.16 to 1.08 at the cost of increasing their fluctuations. In practice, this property can be utilized by an variant of STDMA that has control slots and data slots, such as those in [32, 33, 34]. For example, if an variant similar to that in [34] is considered, the scheduling variables p_k obtained can be regarded as the probabilities to select a feasible schedule in the control slots. Then, if a link knows whether it is included in the schedule, it can determine its state in the data slots based on the control information. Given that, we can apply this algorithm to the wireless network we have at any time, optimal or otherwise, and continue doing so while it progresses on the convergence under a limited number of iterations. In other words, our MLCLOP-DA on the STDMA variants can adopt the parameters obtained within the time constraint and have the characteristic of the programming-based optimization noted in [35] that is not necessary to wait until the algorithm has converged before transmission.

Apart from the above practical issue, we still have a trade-off between MLCLOP-LP and MLCLOP-DA in terms of communication costs and possible benefits of a distributed algorithm, and the similar trade-off may exist for any mechanism in the networking that has both centralized algorithms and distributed counterparts. To be specific, we note that a sensor network can also involve a base station in addition to a large number of sensor stations, such as that considered in [33]. In the network, a base station may have the transmission range much larger than that of sensor stations. In this case, our VMIMO-CB can be utilized to periodically report the data of vnodes to the base station through multi-hop transmissions. Then, after collecting all the necessary information, the base station will carry out MLCLOP-LP, and broadcast the lifetime and scheduling parameters resulted to its vnodes via only one hop. That is, in the case where the cost of multi-hop transmissions is less than that of local transmissions between vnodes, and the base station is equipped with an energy supply and a high gain antenna, MLCLOP-LP may be preferred. On the other hand, if a STDMA variant with control and data slots considered in the above is adopted and no base station is involved, MLCLOP-DA would be preferred to prolong the network lifetime that can be realized or approximated with a limited number of iterations.

7.3. **Comparison results.** To confirm our objective on the lifetime, we compare our MLCLCP-CG with MESP in [19] that minimizes the energy consumed per packet under a similar ground of this work. For the comparison, we adopt the regular topology in Section 7.1, and the DPDR transmission scheme of 8 powers and 4 rates in Table 3, with

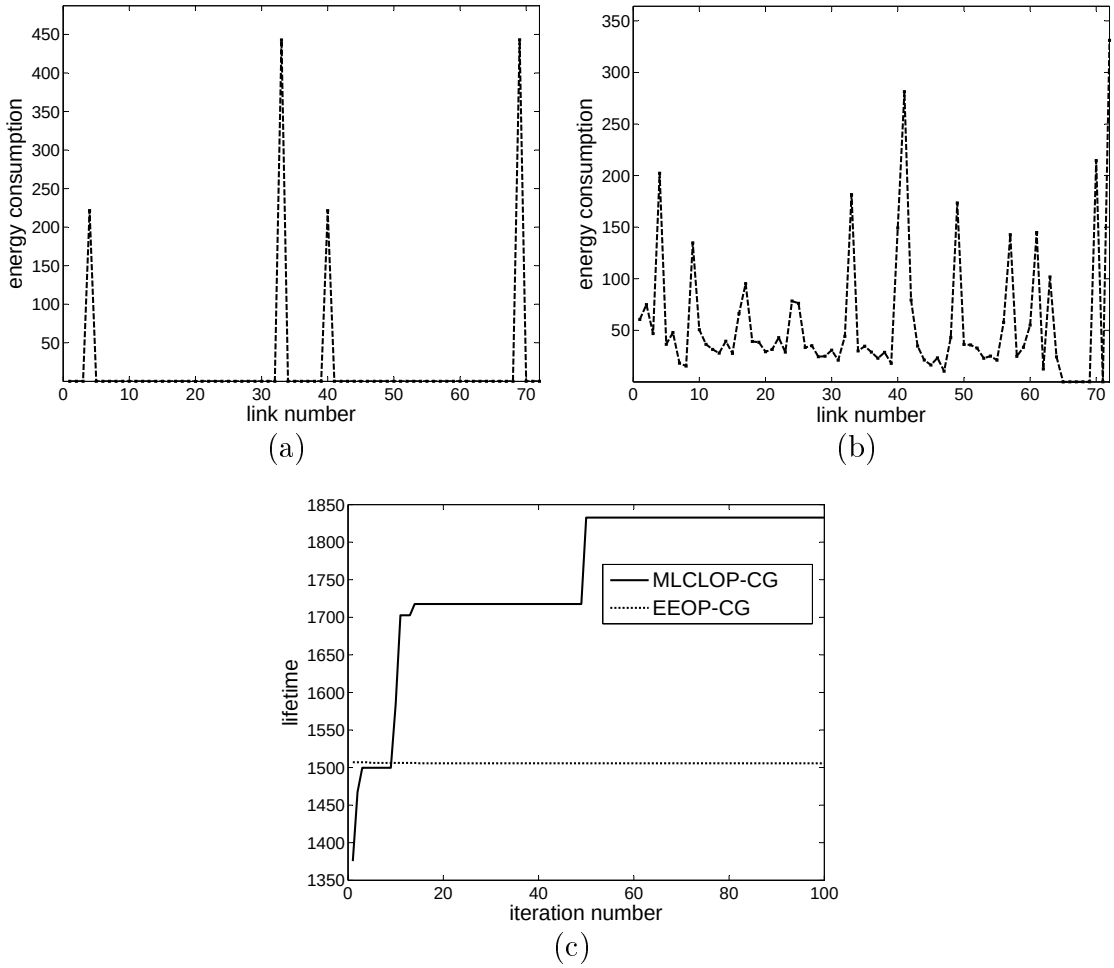

FIGURE 7. Comparison results: (a) energy consumption of MESP, (b) energy consumption of MLCLOP-CG, and (c) lifetime results

the initial energy of 10^6 units. Then, we conduct two sessions, $\{s_1 = 1, d_1 = 9\}$, $\{s_2 = 9, d_2 = 1\}$, with their traffic loads $TL_1 \approx 17.407$ Kbps and $TL_2 = 2 \times TL_1 \approx 34.814$ Kbps imposed on the different optimizations.

The results are given in Figure 7. As one may expect, making a schedule that can minimize the energy consumption per packet would improve the overall energy efficiency in the network, and thus could be beneficial to the time to network partition (i.e., the network lifetime). This is confirmed by Figure 7(c) showing that the lifetimes of MESP is actually high enough throughout the iterations. However, as expected also, if all the traffic is routed through the minimum energy path to the destination, the vnodes in that path will be drain-out of batteries quickly while other vnodes, which perhaps will be more power hungry if traffic is forwarded through them, will remain intact. Apparently, it is shown in Figure 7(a) that after 100 CG iterations, MESP converges to its four most energy efficient links to carry out the whole traffic loads, and the column generation cannot further increase the network lifetime, and only remain the same value at the beginning. In contrast to the above, it is shown in Figure 7(b) that MLCLOP-CG can more evenly distribute the traffic load to the other links in addition to the most energy efficient links, and hence, can gradually increase the network lifetime with the column generation approach. This indeed verifies the design implication of our cross-layer optimization that in order to maximize the lifetime, the traffic should be routed such that the energy consumption is balanced

among the vnodes in proportion to their energy reserves, instead of routing to minimize the absolute consumed power.

8. **Conclusion.** In this work, we have shown a cross-layer formulation to jointly address routing, link scheduling, and rate control in such networks with the aim of finding the most energy-efficient scheduling that can maximize the network lifetime while satisfying the end-to-end traffic demand for a set of source-destination pairs in the wireless sensor networks with VMIMO-CB transmission. In particular, we have exhibited how the most realistic model taking into account discrete power and discrete rate can be incorporated into our formulation. This allows us to gain insights in the influence of discrete power/rate control, spatial reuse, routing strategy and session load distribution on the network performance. Specifically, we have developed a specialized solution based on linear programming along with a column generation approach that is represented by an integer programming formulation, and demonstrated the approach in the computational examples within a reasonable time constraint. In addition, we have developed a fully distributed algorithm using the Lagrangian duality and a subgradient method to allow each node to independently obtain its own lifetime and scheduling variables. The numerical experiment results readily showed that the proposed cross-layer optimization is capable on achieving the network lifetime maximization, and on providing valuable viewpoints on the linear/convex programming-based optimization and its distributed counterpart.

Acknowledgment. This work was supported by the National Science Council, Taiwan, under grant NSC100-2221-E-126-004.

REFERENCES

[1] H. Ochiai, P. Mirtan and H. V. Poor, Collaborative beamforming for distributed wireless ad hoc sensor networks, *IEEE Transactions on Signal Process*, vol.53, no.11, pp.4110-4124, 2005.

[2] R. Mudumbai, D. R. Brown, U. Madhow and H. V. Poor, Distributed transmit beamforming: Challenges and recent progress, *IEEE Communications Magazine*, vol.47, no.2, pp.102-110, 2009.

[3] M. F. Ahmed and S. A. Vorobyov, Collaborative beamforming for wireless sensor networks with Gaussian distributed sensor nodes, *IEEE Transactions on Wireless Communications*, vol.8, no.2, pp.638-643, 2009.

[4] N. Bambos, Toward power-sensitive network architectures in wireless communications: Concepts, issues, and design aspects, *IEEE Personal Communications*, vol.5, no.3, pp.50-59, 1998.

[5] M. Xiao, N. B. Shroff and E. K. P. Chong, A utility-based power-control scheme in wireless cellular systems, *IEEE/ACM Transactions on Networking*, vol.11, no.2, pp.210-221, 2003.

[6] A. El Gamal, C. Nair, B. Prabhakar, E. Uysal-Biyikoglu and S. Zahedi, Energy-efficient scheduling of packet transmissions over wireless networks, *Proc. of the 21st Annual Joint Conference of the IEEE Computer and Communications Societies, INFOCOM'02*, vol.3, pp.1773-1782, 2002.

[7] Y. Yao and G. B. Giannakis, Energy-efficient scheduling for wireless sensor networks, *IEEE Transactions on Communications*, vol.53, no.8, pp.1333-1342, 2005.

[8] T. ElBatt and A. Ephremides, Joint scheduling and power control for wireless ad-hoc networks, *Proc. of the 21st Annual Joint Conference of the IEEE Computer and Communications Societies, INFOCOM'02*, vol.2, pp.976-984,2002.

[9] S. Cui, A. Goldsmith and A. Bahai, Joint modulation and multiple access optimization under energy constraints, *IEEE Global Telecommunications Conference, GLOBECOM'04*, vol.1, pp.151-155, 2004.

[10] J.-H. Chang and L. Tassiulas, Maximum lifetime routing in wireless sensor networks, *IEEE/ACM Transactions on Networking*, vol.12, no.4, pp.609-619, 2004.

[11] R. Madan and S. Lall, Distributed algorithms for maximum lifetime routing in wireless sensor networks, *IEEE Transactions on Wireless Communications*, vol.5, no.8, pp.2185-2193, 2006.

[12] M. Cheng, X. Gong and L. Cai, Joint routing and link rate allocation under bandwidth and energy constraints in sensor networks, *IEEE Transactions on Wireless Communications*, vol.8, no.7, pp.3770 -3779, 2009.

[13] R. L. Cruz and A. V. Santhanam, Optimal routing, link scheduling and power control in multihop wireless networks, *The 22nd Annual Joint Conference of the IEEE Computer and Communications Societies, INFOCOM'03*, vol.1, pp.702-711, 2003.

[14] R. Madan, S. Cui, S. Lal and A. Goldsmith, Cross-layer design for lifetime maximization in interference-limited wireless sensor networks, *IEEE Transactions on Wireless Communications*, vol.5, no.11, pp.3142-3152, 2006.

[15] H. Wang, Y. Yang, M. Ma, J. He and X. Wang, Network lifetime maximization with cross-layer design in wireless sensor networks, *IEEE Transactions on Wireless Communications*, vol.7, no.10, pp.3759-3768, 2008.

[16] M. Johanssom and L. Xiao, Cross-layer optimization of wireless networks using nonlinear column generation, *IEEE Transactions on Wireless Communication*, 2006.

[17] S. Kompella, J. E. Wieselthier and A. Ephremides, Multi-hop routing and scheduling in wireless networks subject to sinr constraints, *The 46th IEEE Conference on Decision and Control*, pp.5690-5695, 2007.

[18] R. Bhatia and M. Kodialam, On power efficient communication over multi-hop wireless networks: Joint routing, scheduling and power control, *The 23rd Annual Joint Conference of the IEEE Computer and Communications Societies, INFOCOM'04*, vol.2, pp.1457-1466, 2004.

[19] J.-S. Liu, An energy-efficient transmission scheme for cooperative MIMO wireless networks, *Proc. of International Conference on Wireless Networks*, pp.251-257, 2011.

[20] M. F. A. Ahmed and S. A. Vorobyov, Node selection for sidelobe control in collaborative beamforming for wireless sensor networks, *IEEE the 10th Workshop on Signal Processing Advances in Wireless Communications*, pp.519-523, 2009.

[21] K. Hardwick, D. Goeckel, D. Towsley, K. Leung and Z. Ding, Antenna beam pattern model for cooperative ad-hoc networks, *ACITA'08*, pp.435-445, 2008.

[22] C. A. Balanis, *Antenna Theory*, 3rd Edition, John Wiley and Sons, Inc., 2005.

[23] S. Cui, A. J. Goldsmith and A. Bahai, Energy-efficiency of MIMO and cooperative MIMO techniques in sensor networks, *IEEE Journal on Selected Areas in Communications*, vol.22, no.6, pp.1089-1098, 2004.

[24] G. Kramer, M. Gastpar and P. Gupta, Cooperative strategies and capacity theorems for relay networks, *IEEE Transactions on Information Theory*, vol.51, no.9, pp.3037-3063, 2005.

[25] R. Nelson and L. Kleinrock, Spatial-TDMA: A collision-free multihop channel access control, *IEEE Transactions on Communications*, vol.33, pp.934-944, 1985.

[26] J. Zhang, H. Wu, Q. Zhang and B. Li, Joint routing and scheduling in multi-radio multi-channel multi-hop wireless networks, *The 2nd International Conference on Broadband Networks (BroadNets'05)*, vol.1, pp.631-640, 2005.

[27] P. Bjorklund, P. Varbrand and D. Yuan, Resource optimization of spatial TDMA in ad hoc radio networks: A column generation approach, *IEEE INFOCOM'03*, pp.818-824, 2003.

[28] M. Kohvakka, M. Kuorilehto, M. Hannikainen and T. D. Hamalainen, Performance analysis of IEEE 802.15.4 and Zigbee for large-scale wireless sensor network application, *PE-WASUN'06*, pp.48-57, 2006.

[29] S. Cui, A. J. Goldsmith and A. Bahai, Modulation optimization under energy constraints, *IEEE International Conference on Communications*, vol.4, pp.2805-2811, 2003.

[30] Draft amendment to ieee std 802.11, 1999 edition (reaff 2003) amendment 7: 4.9 ghz5 ghz operation in japan (as amended by ieee stds 802.11a-1999, 802.11b-1999, 802.11b-1999/cor 1-2001, 802.11d-2001, 802.11g-2003, 802.11h-2003, and 802.11i-2004), *IEEE Std P802.11j/D1.6*, 2007.

[31] Approved draft revision for ieee standard for information technology-telecommunications and information exchange between systems-local and metropolitan area networks-specific requirements-part 15.4b: Wireless medium access control (mac) and physical layer (phy) specifications for low rate wireless personal area networks (wpans) (amendment of ieee std 802.15.4-2003), *IEEE Std P802.15.4/D6*, 2006.

[32] H. Lans, Position indicating system, *US Patent 5506587*, 1996.

[33] Y. Wang, I. Henning, X. Li and D. Hunter, SOTP: A self-organized TDMA protocol for wireless sensor networks, *Proc. of IEEE CCECE/CCGEI*, pp.1108-1111, 2006.

[34] J. Ni, B. Tan and R. Srikant, Q-CSMA: Queue-length based CSMA/CA algorithms for achieving maximum throughput and low delay in wireless networks, *Proc. of IEEE INFOCOM'10*, pp.271-275, 2010.

[35] T. Ho and D. S. Lun, *Network Coding: An Introduction*, Cambridge University Press, 2008.